Journal of Alloys and Compounds 505 (2010) 787–792

Contents lists available at ScienceDirect

Journal of Alloys and Compounds

journal homepage: www.elsevier.com/locate/jallcom

Optical and electrical transport properties of spray deposited $CdS_{1-x}Se_x$ thin films

A.A. Yadav*, E.U. Masumdar

Thin Film Physics Laboratory, Department of Physics, Electronics and Photonics, Rajarshi Shahu Mahavidyalaya, Latur, M.S. 413512, India

ARTICLE INFO

Article history:
Received 29 March 2010
Received in revised form 17 June 2010
Accepted 22 June 2010
Available online 1 July 2010

Keywords:
Thin films
Chemical synthesis
Optical properties
Electrical transport

ABSTRACT

$CdS_{1-x}Se_x$ thin films with different compositions have been deposited on amorphous glass substrates by spray pyrolysis technique. The spectrum shows a sharp fall in absorbance at wavelength corresponding to the band gap of the material. The optical band gap has been determined for all compositions and found to be direct allowed. The band gap has been observed to strongly depend on the film composition. The electrical conductivity of the deposited films has been studied as a function of temperature. All the films showed a transition from phonon-assisted hopping conduction through the impurity band to grain boundary limited conduction in the conduction/valence band at temperature around 370 K. The conductivity is found to vary with composition. The activation energies of the films of different compositions determined at low and high-temperature region have been observed to be in the range 0.113–0.323 eV. The Hall effect studies carried out on the deposited thin films reveal that films exhibit n-type of conductivity. The carrier concentration has been determined from Hall effect studies and is of the order of 10^{15} cm^{-3}.

1. Introduction

The II–VI semiconductor compounds such as CdS, CdSe, CdTe, $Cd_{1-x}Zn_xS$ and $CdS_{1-x}Se_x$, belonging to cadmium chalcogenides family are considered to be very important materials for wide spectrum of opto-electronic applications as having specific physical properties such as direct band gap, high coefficient of absorption in visible and IR region of spectrum, good electrical properties and increased capability in obtaining p- or n-type conductivity by doping. The cadmium chalcogenides have widely contributed to the phenomenal growth of their applications in scientific, technological and industrial applications like solar cells [1–3], photocatalysis [4], field effect transistors [5], opto-electronic devices [6,7] and photo assisted decomposition of water [8]. CdS and CdSe are two very important wide band gap semiconductors, because of their wide applications in opto-electronics, such as non-linear optics, visible light emitting diodes and lasers [1,9]. Particularly, the visible and near infrared band gaps of CdSe (1.74 eV) and CdS (2.44 eV) make them potential candidates for the conversion of low energy photons into electricity. The alloy of Cd–S–Se should have more applications since its band gap can be tuned by means of the changing composition of the elements. However, for the efficient opto-electronic device application, material is usually between CdS in which very high sensitivity is possible but response time is high and CdSe in which a lower response time is possible at the cost of some loss in sensitivity.

In past II–VI thin films have been prepared by different deposition techniques like electrodeposition [1,10] chemical bath deposition [10–13], vacuum evaporation [14,15], pulse plating [16], and chemical spray pyrolysis [17,18]. Among these various deposition techniques available for preparation of thin films, the spray pyrolysis, which has the advantages of low cost, easy-to-use, safe and can be implemented in a standard laboratory, has been known to be suitable for many scientific studies and technological applications. This method is based on the preparation of solutions of some salt of the material whose films are to be prepared.

Shahane et al. [11] have studied the electrical and optical properties of mixed Cd–S–Se thin films prepared by chemical bath deposition. Chaudhari et al. [13] have studied the growth and characterization of ternary Cd–S–Se alloy thin films for opto-electronic applications. Mane et al. [19] have studied photosensitization of nanocrystalline TiO_2 film electrode with cadmium sulphoselenide thin films. Even though a lot of research is being pursued on Cd–S–Se thin films and reports are available on the structural, compositional and optical properties of $CdS_{1-x}Se_x$ thin films, not many reports are available on the opto-electronic properties and practically no report is available on the optical and electrical transport properties of spray deposited $CdS_{1-x}Se_x$ thin films. In this paper we present the optical and electrical transport properties of spray deposited $CdS_{1-x}Se_x$ ($0.0 \le x \le 1.0$) thin films.

2. Experimental

The spray pyrolysis method is basically a chemical deposition technique in which fine droplets of the desired material are sprayed onto a preheated substrate. Continuous films are formed on the hot substrate by thermal decomposition of the material droplets. $CdS_{1-x}Se_x$ thin films were deposited onto glass substrates by

* Corresponding author. Tel.: +91 9975213852.
E-mail address: aay_physics@yahoo.co.in (A.A. Yadav).

0925-8388/$ – see front matter © 2010 Elsevier B.V. All rights reserved.
doi:10.1016/j.jallcom.2010.06.141

spray pyrolysis method. 0.025 M aqueous solutions of cadmium chloride dehydrate ($CdCl_2{\cdot}2H_2O$), thiourea ($(NH_2)_2CS$) and selenourea ($(NH_2)_2CSe$) were used as starting materials. The temperature of substrate was controlled by an iron–constantan thermocouple and kept constant at its optimized value of 300 °C [18]. The spray rate employed was 3 ml/min and kept constant throughout the experiment. The nozzle to substrate distance was 30 cm. After deposition, the films were allowed to cool at room temperature. The adhesion of the films onto the substrates was quite good.

The thickness of thin film was determined using gravimetric weight difference method with sensitive microbalance by assuming bulk density of corresponding materials. The optical absorption spectra were recorded from 350 to 850 nm wavelength using SHIMADZU UV-1700 UV–vis spectrophotometer at room temperature. The absorption coefficient, forbidden energy gap and type of transition were determined from these studies. A DC two point probe method was employed to measure electrical conductivity of the samples. The working temperature was in the range of 300–500 K. Hall Effect setup supplied by Holmarc Opto-Mechatronics Pvt. Ltd. Cochin, India was used for measurements of carrier concentration (n) and Hall mobility (μ) at room temperature. Van der Pauw technique [20] was used for this purpose. Specially designed Hall probe on printed circuit board (PCB) was used to fix the sample of the size $10 \times 10\,mm^2$. Silver paste was employed to ensure good electrical contacts.

3. Results and discussion

In general CdS and CdSe exist in two crystal structures, namely, Wurtzite (cubic) and zinc blende (hexagonal). It has been reported that chemically deposited CdS and CdSe films depending upon preparative conditions, show cubic, hexagonal or mixed (cubic + hexagonal) crystal structures. X-ray diffraction patterns of spray deposited $CdS_{1-x}Se_x$ ($0 \le x \le 1$) thin films are depicted elsewhere [18]. It is seen that all samples are polycrystalline over entire range of composition parameter. For $x = 0.0$ (CdS), the preferential orientation is along (1 0 0), (0 0 2), (1 0 1), (1 1 0) and (1 1 2) planes as matched with the standard JCPDS data card 77-2306 of CdS hexagonal crystal structure. The dominant peaks (1 0 0), (0 0 2), (1 0 1) and (1 1 0) shift towards the lower 2θ side, thereby increasing their d-values: from 3.5418 to 3.6833 Å for (1 0 0) plane, from 3.3332 to 3.4631 Å for (0 0 2) plane, from 3.1311 to 3.2661 Å for (1 0 1) plane and from 2.0587 to 2.1337 Å for (1 1 0) plane respectively with increase in composition parameter x. From XRD patterns it is observed that $CdS_{1-x}Se_x$ ($0 < x < 1$) thin films are composed of mixed crystallites of both CdS and CdSe. The crystallographic phases of samples are in good agreement with the typical hexagonal crystal structure [21,22]. In addition the diffraction peaks for (1 1 0) are located at 43.94°, 43.78°, 43.36°, 42.96°, 42.62° and 42.32°, respectively. The shifting of peak position with increase in the composition 'x' suggests the formation of alloy system in between CdS and CdSe compounds. For $x = 1.0$ (CdSe), the preferential orientation is along (1 0 0), (0 0 2), (1 0 1), (1 1 0), (1 1 2), (2 0 2), (2 0 3), and (3 0 0) planes as matched with the standard JCPDS data card 77-2307 of CdSe [22]. Films with crystallite size in the range of 13–18 nm can be obtained. SEM studies showed polycrystalline texture with nearly smooth surface and clearly defined grains. EDAX study confirmed nearly stoichiometric deposition of $CdS_{1-x}Se_x$ thin films [18].

3.1. Optical studies

The study of the materials by means of optical absorption provides a simple method for explaining some features concerning the band structure and energy gap of non-metallic materials. Optical measurements constitute the most important means of determining the band structures of semiconductors. The optical absorption spectra of spray deposited $CdS_{1-x}Se_x$ ($0.0 \le x \le 1.0$) thin films have been used to evaluate the coefficient of absorption, optical band gap, and nature of transition involved. The wavelength dependence of the absorption coefficient is shown in Fig. 1. It is found that the optical absorption coefficient is high for all the compositions ($\alpha = 10^4\,cm^{-1}$). The absorption through film is relatively high at below band gap region indicating high concentration of defects

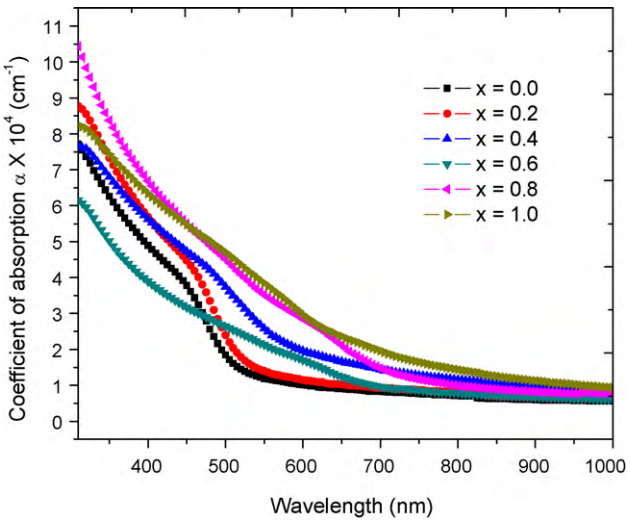

Fig. 1. Variation of coefficient of absorption (α) with wavelength (nm) for spray deposited $CdS_{1-x}Se_x$ ($0.0 \le x \le 1.0$) thin films.

and free carriers. The absorption decreases abruptly in the long wavelength region. The sharp decrease in absorption is observed in between 510 and 710 nm which is due to band edge absorption. A shift in absorption edge from 510 to 710 nm is observed as x is increased from 0 to 1. The incoming photons have sufficient energy to excite electrons from the valence band to the conduction band, resulting in strong absorption in $CdS_{1-x}Se_x$ ($0.0 \le x \le 1.0$) thin films. The optical absorption data are further analysed for near edge optical absorption of semiconductor by using the following relationship [23],

$$\alpha h\nu = A(h\nu - E_g)^m \quad (1)$$

where α is coefficient of absorption, A is an energy-independent constant and E_g is the optical band gap energy. The exponent m depends on the nature of the transition, $m = 1/2$, 2, 3/2 or 3 for allowed direct, allowed indirect, forbidden direct or forbidden indirect transitions, respectively. Now for allowed direct type of transitions Eq. (1) can written as

$$\alpha h\nu = A(h\nu - E_g)^{1/2} \quad (2)$$

Thus a plot of $(\alpha h\nu)^2$ vs. $h\nu$ is a straight line whose intercept on energy axis gives the band gap energy, E_g as shown in Fig. 2. The straight line nature of the plots over a wide range of photon energy indicates the direct allowed type of transition. It is well known that direct transition across the band gap is feasible between the valence and conduction band edges in k space. In the transition process, the total energy and momentum must be conserved. The optical gaps have been then determined by the extrapolation of the linear regions on energy axis. The variation of band gap with composition is shown in Fig. 3. The band gap is found to decrease from 2.44 eV corresponding to CdS to 1.74 eV corresponding to CdSe with increase in Se concentration. The obtained band gap in the present case matches well with the reported values of CdS [24] and CdSe [25]. The other compositions have in between values. The results show that band gap varies smoothly but not linearly over the entire range of composition studied. The non-linearity of the band gap variation with compositions has been already reported for $Cd_{1-x}Zn_xS$ [26,27], CdS–Bi_2S_3 [28], CdSSe [13] and also for quaternary $CdZn(S_{1-x}Se_x)_2$ [29] thin films. The reason for this behavior in the present study may be attributed to slight variation in film composition than bulk composition and thickness. Such a kind of broad and fine variation/tunable band gap properties of ternary alloy $CdS_{1-x}Se_x$ thin films are suitable for many

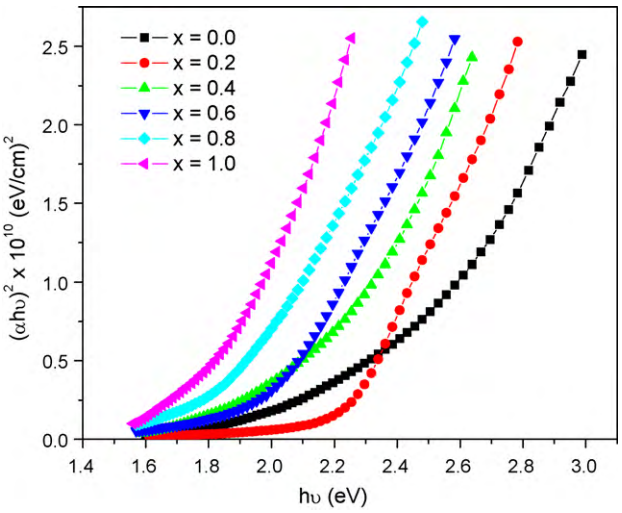

Fig. 2. Variation of $(\alpha h\nu)^2$ with $h\nu$ for spray deposited $CdS_{1-x}Se_x$ ($0.0 \le x \le 1.0$) thin films.

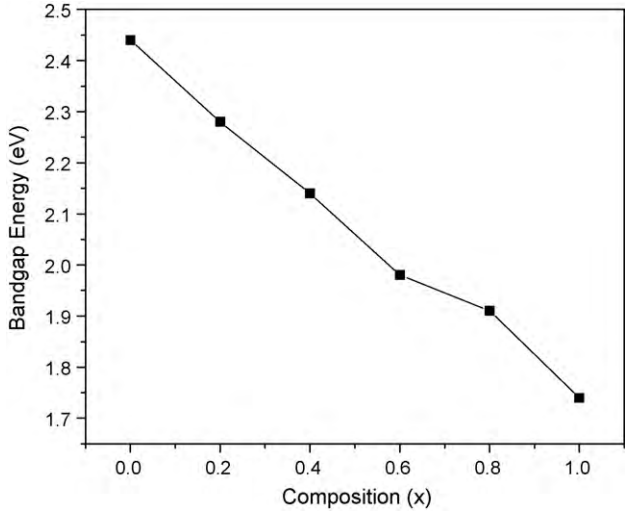

Fig. 3. Variation of band gap energy (eV) with composition for spray deposited $CdS_{1-x}Se_x$ ($0.0 \le x \le 1.0$) thin films.

scientific studies and technological applications such as gas sensors, heat mirrors, transparent electrodes, solar cells, piezoelectric and opto-electronic devices.

The curves in the plots $(\alpha h\nu)^{2/3}$ vs. $h\nu$ (direct forbidden), $(\alpha h\nu)^{1/2}$ vs. $h\nu$, (indirect allowed) and $(\alpha h\nu)^{1/3}$ vs. $h\nu$ (indirect forbidden) can not be extrapolated to the energy axis. These plots (not shown) reveal that the type of transition is neither direct forbidden nor indirect. The modes of optical transitions in these films have also been determined as suggested by Pal and co-workers [30]. Eq. (1)

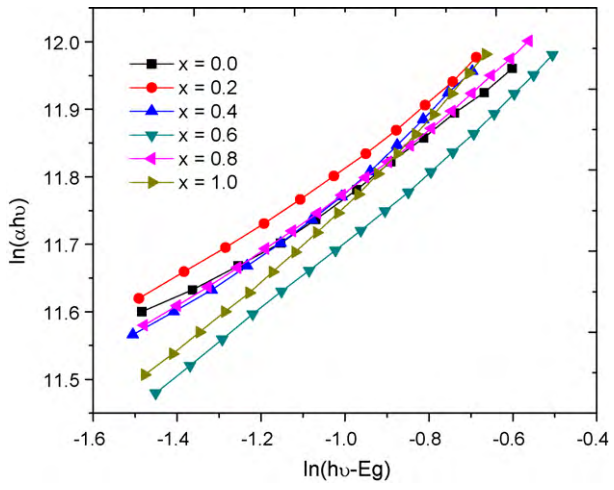

Fig. 4. Evaluation of mode of transition from the variation of $\ln(\alpha h\nu)$ vs. $\ln(h\nu - E_g)$ for spray deposited $CdS_{1-x}Se_x$ ($0.0 \le x \le 1.0$) thin films.

can be rearranged as

$$\ln(\alpha h\nu) = \ln(A) + m\,\ln(h\nu - E_g) \quad (3)$$

and suggests that the plot of $\ln(\alpha h\nu)$ vs. $\ln(h\nu - E_g)$ is a straight line whose slope gives the power factor m. Fig. 4 indicates the results of above analysis and the calculated values of m for all the compositions are given in the Table 1. The obtained values of m suggest that the fundamental absorption edge in the films is formed by the direct allowed transitions.

3.2. Electrical transport studies

The electrical characterization of the as deposited $CdS_{1-x}Se_x$ thin films were carried out by the means of the temperature dependent conductivity and Hall effect measurements in the temperature range 300–500 K. Fig. 5 shows the temperature dependence of DC electrical conductivity of $CdS_{1-x}Se_x$ thin films. From Fig. 5 it is seen that the curves are linear and electrical conductivity of all films is found to increase with increase in temperature. The electrical conductivity is found to be composition dependent. The room temperature electrical conductivities for CdS and CdSe are 6.34×10^{-7} and 2.71×10^{-6} $(\Omega\,cm)^{-1}$, respectively. The observed lesser conductivity in thinner films can be explained due to a lower degree of crystallinity and a small grain size. The presence of defects such as structural disorders, dislocations and surface imperfections also play role in decreasing the conductivity as reported earlier [31]. The lower values of electrical conductivity can also be attributed to the deposition method and generally chemical methods result into lower magnitudes of electrical conductivities more low for CdS than CdSe. For in between compositions of CdS and CdSe the electrical conductivity is found to increase with increase in Se content in the film up to $x = 0.8$, thereafter the conductivity decreases. This is due to the fact that $CdS_{1-x}Se_x$ thin films are inhomogeneous semi-

Table 1
Optical and electrical parameters of spray deposited $CdS_{1-x}Se_x$ thin films.

Composition	Thickness (nm)	E_g (eV)	Power factor	Activation energy		Conductivity	Mobility
				LT (eV)	HT (eV)	$\times 10^{-6}$ $(\Omega\,cm)^{-1}$	$(\times 10^{-3})$ $(cm^2\,V^{-1}\,s^{-1})$
CdS	210	2.44	0.4693	0.162	0.276	0.633	1.091
$CdS_{0.8}Se_{0.2}$	201	2.28	0.4471	0.133	0.300	1.122	1.534
$CdS_{0.6}Se_{0.4}$	194	2.14	0.5414	0.113	0.299	2.192	2.400
$CdS_{0.4}Se_{0.6}$	189	1.98	0.5700	0.126	0.310	3.499	3.179
$CdS_{0.2}Se_{0.8}$	183	1.91	0.5244	0.214	0.323	6.166	4.502
CdSe	181	1.74	0.5597	0.192	0.274	2.713	2.709

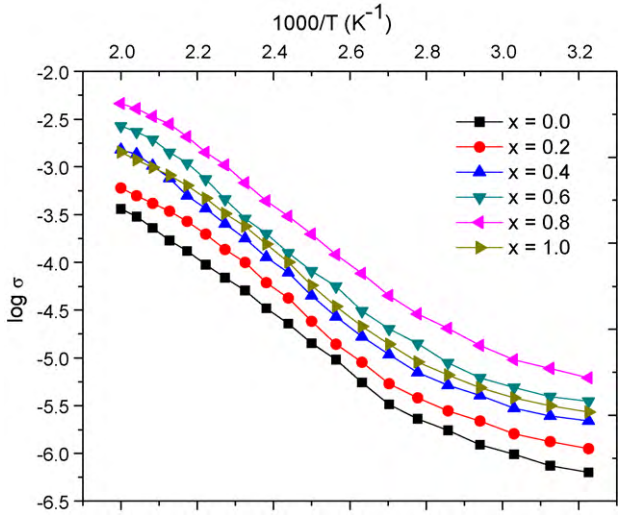

Fig. 5. Plot of $\log\sigma$ vs. $(1000/T)$ for spray deposited $CdS_{1-x}Se_x$ $(0.0 \le x \le 1.0)$ thin films.

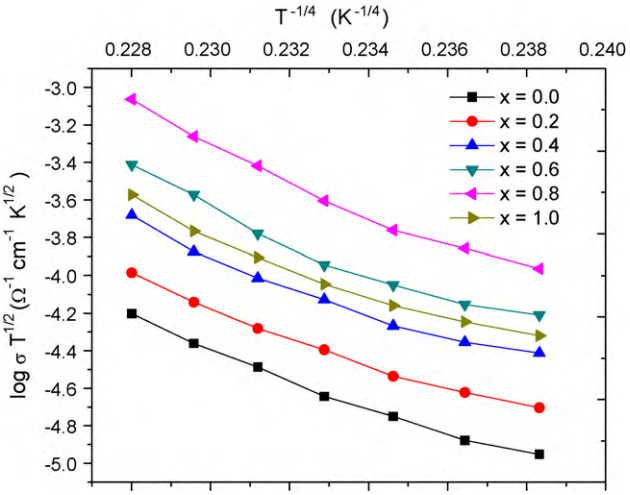

Fig. 6. Variation of $\log(\sigma T^{1/2})$ vs. $T^{-1/4}$ to determine the variable range hopping conduction mechanisms in spray deposited $CdS_{1-x}Se_x$ $(0.0 \le x \le 1.0)$ thin films.

conductors with deep impurity levels possessing large values of potential relief inhomogenity associated with the impurity zone as well as the intrinsic zone [32].

As seen from Fig. 5, the temperature dependent conductivity of the $CdS_{1-x}Se_x$ thin films shows very similar behavior except for the magnitudes over the entire range of the composition. This indicates that the same conduction mechanisms are dominant for all compositions. From Fig. 5, the variation of the conductivity with the temperature for all composition shows two regions with two different activation energies, indicating different conduction mechanisms dominating at specific temperature intervals. In low-temperature regions, between 300 and 370 K, the temperature dependence of conductivity for all composition increases slightly with small activation energies. In low-temperature region, the increase in conductivity with temperature is due to the intrinsic nature of film. In this temperature region, there is no adequate number of charge carriers due to its intrinsic defects and mobility of charge carriers is low. Also at low temperatures, the charge carriers in conduction band may be too few to give rise to an appreciable conduction. Hence hoping of charge carriers via impurity band can result in a current in the films below 370 K. The Mott [23] model may be suitable for explaining the low-temperature electrical conduction in films. According to Mott theory, the electrical conductivity σ due to the hoping of charge carriers via impurity band is given by

$$\sigma = \sigma_0 T^{-1/2} \exp\left[-\left(\frac{T_0}{T}\right)^{1/4}\right] \quad (4)$$

where $\sigma_0 = 3e^2\nu[N(E_f)/8\pi\alpha k]^{1/2}$, $T_0 = \lambda\alpha^3/kN(E_f)$, $N(E_f)$ is the density of states near the Fermi level, λ is a dimensionless constant, ν is the frequency factor taken as the Debye frequency, α is the decay constant of the wave function of localized states near the Fermi level and k is the Boltzmann constant. To confirm the type of conduction mechanism, the plots of $\log(\sigma T^{1/2})$ vs. $T^{1/4}$ have been plotted and are shown in Fig. 6. At low-temperature (<370 K) charge carriers do not have sufficient energy for excitation to the adjacent band and hence they move from one impurity to another with help of phonon.

In high-temperature region, i.e., between the temperatures of 370 and 500 K the variation of conductivity with the inverse of absolute temperature is pronounced and increases sharply with the activation energies in the range 0.274–0.323 eV. At these temperatures, the conductivity increases rapidly with increase in temperature. The low mobility of charge carriers is easily compensated by creation of large number of charge carriers and this result in increase in conductivity of the specimen [33]

From Fig. 5, it is seen that for temperature above 370 K the plot is linearly varying one and the measured experimental data fit well with the relation

$$\sigma(T) = \sigma_0 \exp\left(\frac{-\Delta E_{\sigma 0}}{kT}\right) \quad (5)$$

and therefore the conductivity is attributed to the thermal excitation of charge carriers from grain boundaries to the neutral region of the grains. The activation energies obtained using the $\log\sigma$ vs. $1000/T$ plots are shown in Table 1. The activation energies are in the range 0.113–0.323 eV depending on the film composition, and these values are close to the values reported by Shahane et al. [11]. The activation energy of the films in the low-temperature region (below 370 K) is found to be smaller than the activation energy in the high-temperature region (above 370 K), confirming that the conduction mechanism in the high- and low-temperature regions is a thermally activated process known as thermionic emission and variable range hopping mechanism, respectively.

To confirm the type of conduction mechanism, measurements were analysed by means of the thermionic emission over the grain boundary potential model proposed by Seto [34] where the conductivity is given by

$$\sigma\sqrt{T} = \sigma_0 \exp\left(\frac{-E_a}{kT}\right) \quad (6)$$

where σ_0 is the pre-exponential factor, E_a is the activation energy, k is the Boltzmann constant and T is the absolute temperature. The plots of $\log(\sigma T^{1/2})$ vs. $1000/T$ have been plotted as shown in Fig. 7. Obviously in the high-temperature region, grain boundary limited conduction is dominant conduction mechanism.

As a result of detailed analysis of the temperature dependent conductivity data to obtain the conduction mechanism dominating in the mentioned temperature regions, it was observed that Seto's thermionic emission model is quite applicable as a conduction mechanism in the temperature range 370–500 K (Fig. 7). However, the thermionic conduction mechanism is insufficient to explain the saturation tendency in the low-temperature region below 370 K.

Hence from the above discussion it may be concluded that in spray deposited $CdS_{1-x}Se_x$ thin films there exists a transition temperature around 370 K, above which the electrical conduction is effected by charge carriers excited to the conduction/valence band from impurity levels, and may be explained by Seto's polycrys-

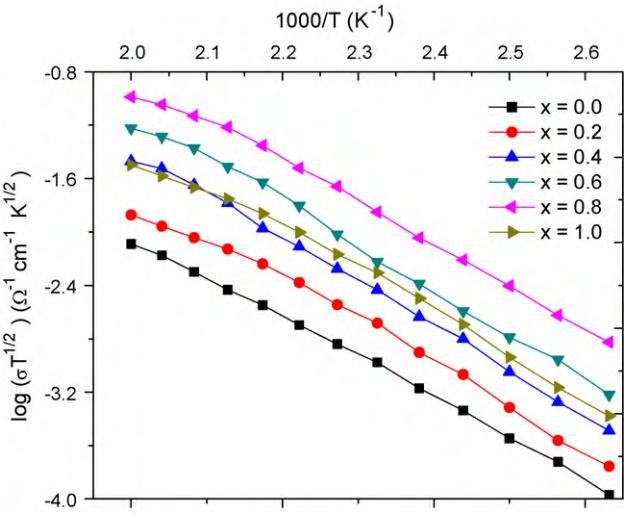

Fig. 7. Variation of $\log(\sigma T^{1/2})$ vs. $1000/T$ to determine the grain boundary limited conduction mechanisms in spray deposited $CdS_{1-x}Se_x$ ($0.0 \le x \le 1.0$) thin films.

talline model of thermionic emission, which is applicable to explain transport phenomena in polycrystalline semiconductor materials. The high-temperature conductivity is attributed to excitation of charge carriers from grain boundaries to neutral region of grains. Below the transition temperature, conduction occurs by phonon-assisted hopping via an impurity band and may be explained by Mott's model.

In order to determine the carrier density and Hall mobility, including the conduction type the Hall effect measurements were carried out on the as deposited $CdS_{1-x}Se_x$ thin films. The Hall effect measurement is the standard, reliable and more direct method for obtaining fundamental electrical properties of semiconductors. Hall effect measurement reveals that the value of Hall coefficient is negative which confirms that the deposited films have n-type conductivity. The carrier density at room temperature was determined for all the samples. The variation of carrier density with composition for spray deposited $CdS_{1-x}Se_x$ thin films is shown in Fig. 8. Carrier density for each composition is in the order of 10^{15}–10^{16} cm^{-3}. The carrier density is found to increase with increase in Se concentration up to Se = 0.8 and further it is observed to decrease for Se = 1.0. Similar dependence of carrier concentration on selenium concentration in $CdSe_xTe_{1-x}$ thin films has been reported by Stuckes and Farrell [35]. This also supports the observations from conductivity measurements. The small carrier density is characteristic of compensation type semiconductors involving deep donors or deep acceptors. The deep donors and acceptors could be associated with doubly ionized cadmium interstitials and doubly ionized cadmium vacancies [36]. Moreover, structural defects and grain boundaries, whose number are generally larger in as deposited materials compared to annealed ones, may also be responsible for reducing carrier density, since they are capable of trapping carriers [33]. The Carrier mobility has been calculated using the standard relation,

$$\mu = \frac{\sigma}{ne} \tag{7}$$

The electron mobility is found to be a function of composition. The electron mobility for spray deposited $CdS_{1-x}Se_x$ thin films is in the range of 1.09–4.50×10^{-3} cm^2 V^{-1} s^{-1}. The smaller values of electron mobility are due to presence of grain boundaries and structural defects which cause scattering of charge carriers. The calculated values of electron mobility at room temperature are listed in Table 1.

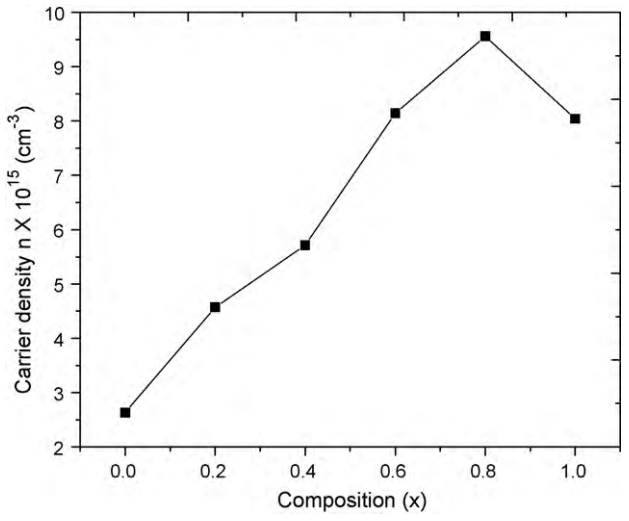

Fig. 8. Variation of carrier density with composition for spray deposited $CdS_{1-x}Se_x$ ($0.0 \le x \le 1.0$) thin films.

4. Conclusions

$CdS_{1-x}Se_x$ thin films have been deposited by spray pyrolysis technique. The optical studies indicated that films exhibit direct bandgap which is strongly dependent on composition allowing tailoring of band gap as required for solar cell applications. The electrical conductivity of $CdS_{1-x}Se_x$ thin films is found to increase with selenium concentration up to $x = 0.8$. The room temperature electrical conductivity for varies in the range of 6.34×10^{-7} and 6.16×10^{-6} $(\Omega\,\text{cm})^{-1}$ depending on the composition of the films. The electrical transport studies reveal that there exists a transition temperature, around 370 K, below which the conduction is due to the variable range hoping mechanism and at temperature above transition temperature the conduction is due to thermionic emission. Hall effect study reveals that all samples are n-type semiconductors. The carrier density of the films is of the order of 10^{15}–10^{16} cm^{-3}. The wide and fine tunability of the band gap as well as the uneven changes in the conductivity of the ternary $CdS_{1-x}Se_x$ thin films have potential applications in various opto-electronic devices.

Acknowledgement

One of the authors A.A. Yadav is grateful to the University Grants Commission, New Delhi (West regional office, Pune), India for the financial assistance through the minor research Project no. F. 47-656/2008.

References

[1] S.M. Pawar, A.V. Moholkar, P.S. Shinde, K.Y. Rajpure, C.H. Bhosale, J. Alloys Compd. 459 (2008) 515.
[2] A.A. Yadav, E.U. Masumdar, Sol. Energy 84 (2010) 1445.
[3] J.K. Dongre, M. Ramrakhiani, J. Alloys Compd. 487 (2009) 653.
[4] M. Esmaili, A. Habibi-Yangjeh, J. Alloys Compd. 496 (2010) 650.
[5] R. Navamathavan, Chi Kyu Choi, Seong-Ju Park, J. Alloys Compd. 475 (2009) 889.
[6] A.S. Khomane, P.P. Hankare, J. Alloys Compd. 489 (2010) 605.
[7] A.S. Khomane, J. Alloys Compd. 496 (2010) 508.
[8] S. Velumani, X. Mathew, P.J. Sebastian, Sol. Energy Mater. Sol. Cells 76 (2003) 359.
[9] A.A. Yadav, M.A. Barote, E.U. Masumdar, Sol. Energy 84 (2010) 763.
[10] S.D. Chavhan, R.S. Mane, T. Ganesh, Wonjoo Lee, Sung-Hwan Han, S. Senthilarasu, Soo-Hyoung Lee, J. Alloys Compd. 474 (2009) 210.
[11] G.S. Shahane, B.M. More, C.B. Rotti, L.P. Deshmukh, Mater. Chem. Phys. 47 (1997) 263.

[12] Fangyang Liu, Yanqing Lai, Jun Liu, Bo Wang, Sanshuang Kuang, Zhian Zhang, Jie Li, Yexiang Liu, J. Alloys Compd. 493 (2010) 305.
[13] J.B. Chaudhari, N.G. Deshpande, Y.G. Gudage, A. Ghosh, V.B. Huse, R. Sharma, Appl. Surf. Sci. 254 (2008) 810.
[14] D. Pathinettam Padiyan, A. Marikani, K.R. Murali, J. Alloys Compd. 365 (2004) 8.
[15] K. Prabakar, Sa.K. Narayandass, D. Mangalaraj, J. Alloys Compd. 364 (2004) 23.
[16] K.R. Murali, P. Thirumoorthy, C. Kannan, V. Sengodan, Sol. Energy 83 (2009) 14.
[17] Saliha Ilican, Yasemin Caglar, Mujdat Caglar, Fahrettin Yakuphanoglu, J. Alloys Compd. 480 (2009) 234.
[18] A.A. Yadav, M.A. Barote, P.M. Dongre, E.U. Masumdar, J. Alloys Compd. 493 (2010) 179.
[19] R.S. Mane, C.D. Lokhande, V.V. Todkar, Hoeil Chung, M.Y. Yoon, S.H. Han, Appl. Surf. Sci. 253 (2007) 3922.
[20] L.J. Van der Pauw, Philips. Res. Rep. 13 (1958) 1.
[21] JCPDS Data Card no. 77-2306.
[22] JCPDS Data Card no. 77-2307.
[23] N.F. Mott, E.A. Davis, Electronic Process in Non-Crystalline Materials, Calendron Press, Oxford, 1979.
[24] A.A. Yadav, M.A. Barote, E.U. Masumdar, Solid State Sci. 12 (2010) 1173.
[25] A.A. Yadav, M.A. Barote, E.U. Masumdar, Mater. Chem. Phys. 121 (2010) 53.
[26] S.V. Borse, S.D. Chavan, R. Sharma, J. Alloys Compd. 436 (2007) 407.
[27] L.P. Deshmukh, C.B. Rotti, K.M. Garadkar, P.P. Hankare, B.M. More, D.S. Sutrave, G.S. Shahane, Indian J. Pure Appl. Phys. 35 (1997) 428.
[28] K.M. Gadave, C.D. Lokhande, P.P. Hankare, Mater. Chem. Phys. 38 (1994) 393.
[29] S.D. Chavan, S.V. Bagul, R.R. Ahire, N.G. Deshpande, A.A. Sagade, Y.G. Gudage, R. Sharma, J. Alloys Compd. 436 (2007) 400.
[30] D. Bhattacharya, S. Chaudhari, A.K. Pal, Vacuum 43 (1992) 313.
[31] D.P. Padiyan, A. Marikani, K.R. Murali, Mater. Chem. Phys. 88 (2004) 250.
[32] A.P. Belyaev, I.P. Kalinkin, Thin Solid Films 158 (1988) 25.
[33] R.A. Smith, Semiconductors, First Edition, Cambridge University Press, Cambridge, 1959, P 116.
[34] J.Y.W. Seto, J. Appl. Phys. 46 (1975) 5247.
[35] A.D. Stuckes, G. Farrell, J. Phys. Chem. Solids 25 (1964) 477.
[36] A.E. Rakhshani, Phys. Status Solidi A 169 (1998) 85.